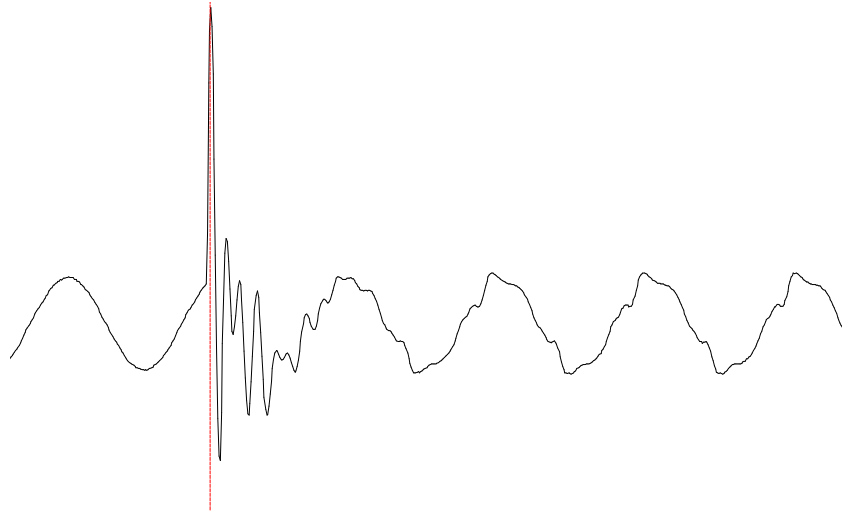


THIS PUBLICATION IS DISTRIBUTED TO MEMBERS ONLY

Harmonics and Transients Tech Notes



Issue # 96-1

March, 1996

Editor: Karen Brown

Project Manager: Susie Brockman

Advisor: Thomas Grebe

in this issue:

Letter from the Electrotek Project Manager:	2
Optimal Capacitor Placement on Radial Distribution Systems to Minimize Harmonic Distortion.....	3
Modeling Relay Operational Characteristics Using the EMTP Program.....	14
Twelve-Pulse Cancellation and DC Motor Drives	27

Letter from Electrotek:

In an effort to better support our members, we have decided to combine the EMTP and HarmFlo+ Tech Notes into one publication. This will make it easier for us to adhere to a regular distribution schedule and will benefit you, the power engineer in exploring two different types of power system analysis. This publication was developed for exchanging information between members of the group. Our members represent varied levels of experience. Currently, technical papers predominate what is being presented but we would invite you to submit other applications of the software such as brief notes on how to tackle a certain problem or situation. We feel the exchange of information is one of the most helpful resources the group can provide. I would like to see the Tech Notes evolve into more of an information exchange and less of merely posting technical papers.

Our Technical Coordinator, Karen Brown, will be serving as editor of this newly combined publication. Many of you who were involved in the EPRI DPQ project will recognize her high efficiency and attention to detail.

Sincerely,

Susie Brockman

For more information concerning the newsletter or to submit a contribution please contact:

Karen Brown
Electrotek Concepts, Inc.
408 North Cedar Bluff Road, Suite 500
Knoxville, Tennessee 37923
Phone: (423) 470-9222 x143 FAX: (423) 470-9223
e-mail: karen@electrotek.com

Optimal Capacitor Placement on Radial Distribution Systems to Minimize Harmonic Distortion

Determining Optimal Locations of Shunt Compensation Capacitors for Radial Distribution Systems with Harmonic Distortion Using a Neighborhood Search Algorithm

Abstract

This paper describes a new method to determine the optimal locations of shunt compensation capacitors for radial distribution systems with harmonic distortion. The state space equations for a network are derived and the network poles and zeros are obtained. The solution to the harmonic resonance problem is formulated as a discrete optimization problem in terms of pole and zero locations. Optimal capacitor locations are determined by means of a neighborhood search algorithm. The procedure is demonstrated on an 18 bus radial distribution network. Furthermore, it is shown that the algorithm does provide optimal harmonic attenuation.

Introduction

Harmonic distortion in the power system is becoming an increasingly important issue in distribution system planning, design and operation. Not only are harmonic levels increasing in distribution systems but consumer loads are also becoming more sensitive to harmonic distortion [1].

Harmonics are generated by a variety of sources, ranging from arc furnaces, drives, transformers, to lighting and computers. Most of these sources inject harmonic currents into the power system. These currents in turn result in harmonic voltage drops across various network elements. In this way harmonics can propagate throughout the power system to buses remote from the harmonic source [2].

If these harmonics are ignored, they can cause harmonic problems such as resonant conditions, telephone interference, capacitor bank failures, overheating of motors, vibrations as well as false tripping of equipment [1].

One way of solving the harmonic distortion problem (HDP) is by making use of sensitivity analysis methods [3, 4]. However, this requires much computational effort since all the system eigenvalues and eigenvectors need to be calculated. In addition, the sensitivity methods rely on a step by step method of analysis whereby the sensitivity factors have to be analyzed for each proposed system configuration.

Recently, the HDP was formulated as an optimization problem [5]. However, the proposed method requires the solution of a three phase load flow at each iteration. This makes the computation cumbersome.

In this paper the HDP is formulated as a discrete optimization problem. The objective function and its constraint are formulated in terms of distances from poles and zeros to the harmonic frequencies. A simple neighborhood search is used to obtain the optimal solution. The method is tested on an 18 bus radial distribution network and the results are presented.

Mathematical Formulation of the HDP

State Space Model

In this study two types of radial distribution systems are considered, namely systems that have a capacitor at the end of each feeder and systems ending with a line on each feeder. The second case can be modeled in the same way as the first case, by modeling the line as part of the load.

In order to derive the state space model for such distribution systems, the independent state variables need to be chosen. These are taken as all the capacitor voltages, as well as all the nodal current injections at buses with capacitors attached to them. The loop and node equations can then be determined and expressed in the familiar state space form:

$$s\mathbf{x} = \mathbf{A}\mathbf{x} + \mathbf{B}\mathbf{u} \quad (\text{eq.1})$$

$$\mathbf{y} = \mathbf{C}\mathbf{x} \quad (\text{eq.2})$$

$$\mathbf{x}^t = [I_1 I_2 \dots I_n V_1 V_2 \dots V_n] \quad (\text{eq.3})$$

where: s is the Laplace operator

x is the $2n \times 1$ state space vector containing the n independent line currents as well as the n independent capacitor voltages

A is the $2n \times 2n$ state coefficient matrix

B is the $2n \times m$ input coefficient matrix

m is the number of harmonic current sources

u is the $m \times 1$ input vector of harmonic source currents

y is the $p \times 1$ voltage output vector

p is the number of nodal output voltages

C is the $p \times 2n$ constant matrix relating the states to the output

I_n is the current injected into node n

V_n is the voltage at node n

Once the state space model has been determined, the parallel resonant frequencies (poles) are obtained by calculating the eigenvalues of the matrix A .

It is well known, that the system transfer function is given by the following [6]:

$$Z(s) = \frac{y}{u} = C \frac{\text{adj}(sI - A)}{\det(sI - A)} B \quad (\text{eq.4})$$

where: $Z(s)$ is the transfer function in the Laplace domain

In the case of a single input, single output system (SISO), where the input is applied at a capacitor node, the system impedance can be rewritten as follows [3]:

$$Z = \frac{1}{C_n} \frac{\det(sI - A_n)}{\det(sI - A)} \quad (\text{eq.5})$$

where: C_n is the capacitance of the capacitor bank at node n

A_n is obtained by eliminating the row and column of A , corresponding to the output node

Thus the series resonant frequencies (zeros) are determined by calculating the eigenvalues of the matrix A_n , which is of dimension $(2n-1) \times (2n-1)$.

Formulation of the HDP as an Optimization Problem

In order to minimize the effect of the HDP, specifications can be placed on the poles and zeros of the system. The zeros should be close to harmonic frequencies and poles should be far from harmonic frequencies unless there is a zero between that pole and the harmonic frequency in question. Furthermore, poles and zeros should be close to each other.

These requirements are formulated as an objective function as follows:

$$\underset{CS}{\text{maximize}}(J = \min_i(\min_j |H_i - P_j|)) \quad (\text{eq.6})$$

Subject to the constraint:

$$C = \min_i(\min_j |H_i - Z_j|) < \mathbf{g} \quad (\text{eq.7})$$

where: H_i the i th harmonic frequency injected by the harmonic source

P_j is the j th system pole

Z_j is the j th system zero

CS is the configuration space or feasibility set [4]

J is the value of the objective function

C is the value of the constraint for the zeros

\mathbf{g} is the limit of the constraint

The configuration space is given by all the possible combinations of capacitor locations. A neighborhood search results when only one capacitor at a time is switched on to another bus, thereby changing two bits in the configuration space.

The formulation of (6) and (7) was chosen, since it is desirable to have the poles far away from a harmonic frequency in order to avoid resonance effects.

Furthermore, by choosing $\mathbf{g} = 1$ it is ensured that there is a zero in the vicinity of a harmonic frequency. This is desirable, as it mitigates the dominance of the harmonic frequency.

Method of Solution

Figure 1 shows a flowchart of the procedure that was used to obtain a solution to the optimization problem as posed in (6) and (7).

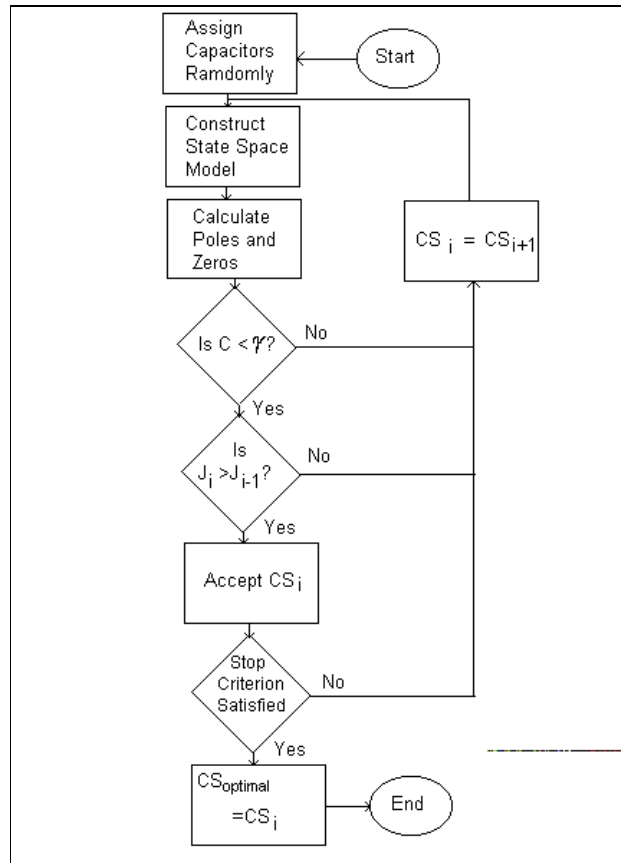


Figure 1: Flowchart of the Optimization Algorithm

After a random initial assignment of capacitors the state space model is generated and the system poles and zeros are calculated. The constraint for the zeros is then checked. If it is not satisfied, a new configuration space element is chosen by changing the position of one capacitor, resulting in a neighborhood search. If the constraint is satisfied, the value of the objective function is calculated and compared to the previous one.

If $J_i < J_{(i-1)}$, a new configuration space element is chosen as explained above. The objective function is once again evaluated and compared to the original value. If $J_i < J_{(i-1)}$, then CS_i is taken as the feasible capacitor assignment.

If $J_i > J_{(i-1)}$, the feasible configuration space element is updated. The process repeats itself until the stop criterion is met. The stop criterion states that if two iterations have not produced an improved J value, the algorithm terminates.

Case Study

The distribution system shown in Figure 2 was studied [3]. The system consists of three feeders connected to a transformer.

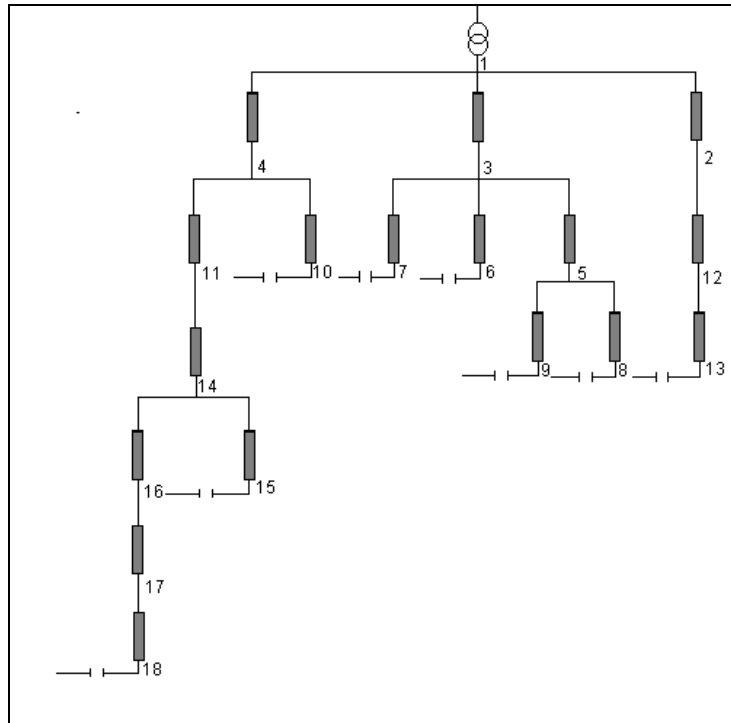


Figure 2: Positive Sequence Representation of the Example Network

The system bases are 1 MVA, 13.2 kV and 377 rad/s. The line data as well as the transformer data is given in Table 1. The capacitor values are all 0.5 per unit. The line resistance and the loads were neglected in the study, as they only have minimal effects on the system poles and zeros thus resulting in a more conservative design. The shunt line capacitance was ignored, as it is negligible compared to the capacitor banks connected to the system.

A 1 MVA 6 pulse converter is connected to bus 18. Only the 5th and 7th harmonic are injected.

The poles and zeros, listed in Table 2, were calculated by using Matlab®. Furthermore, the system response shown in Figure 3, was obtained by using V-Harm®, which was developed by Cooper Industries specifically for harmonic analysis of power systems [8]. The V-Harm® simulation was done by injecting a 0.3 per unit current over all frequencies up to the 10th harmonic.

Table 1: Line and Transformer Data in Percent of Per Unit Values

Line	L	Line	L
Transformer	0.532	5-9	0.127
1-2	0.174	1-4	0.278
2-12	0.246	4-10	0.096
12-13	0.107	4-11	0.171
1-3	1.209	11-14	0.045
3-5	2.968	14-15	0.164
3-6	0.160	14-16	0.251
3-7	2.282	16-17	0.354
5-8	0.055	17-18	0.134

Table 2: Lower System Poles and Zeros in Per Unit Before the Optimization

Poles	Zeros
$\pm j15.3027$	$\pm j35.2219$
$\pm j9.18034$	$\pm j33.3099$
$\pm j7.47741$	$\pm j30.0978$
$\pm j4.11069$	0

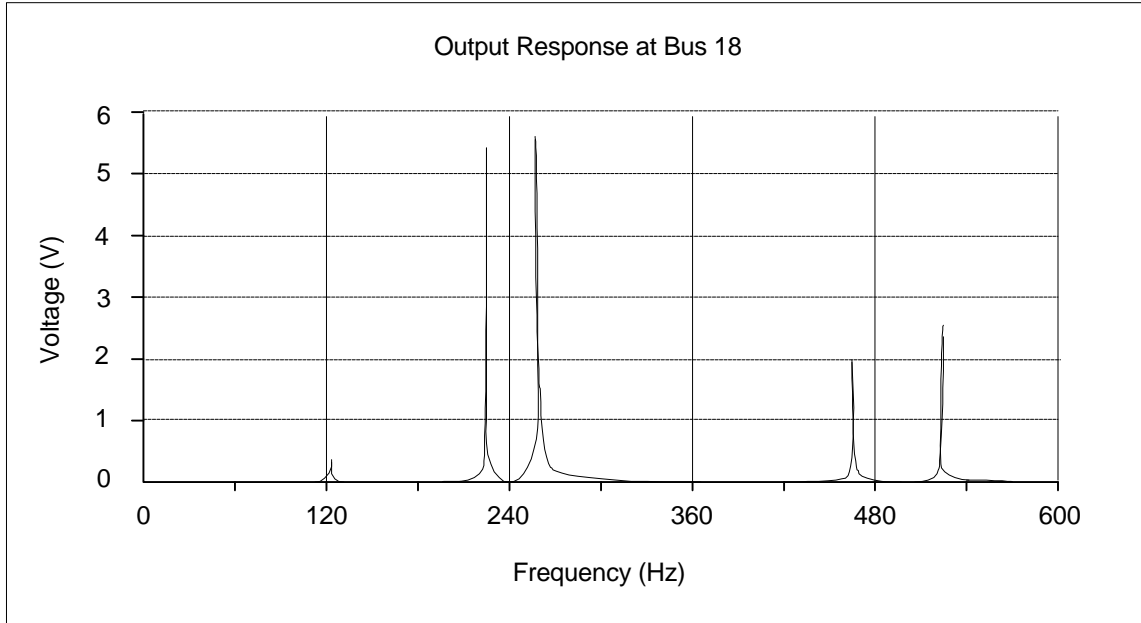


Figure 3: V-Harm® Output Response Before the Optimization

From Table 2 it can be seen that all the zeros are far from the 5th and 7th harmonic. Furthermore, the poles are very close to these frequencies. This indicates that there will be a harmonic distortion problem in the network if no countermeasures are applied. This is confirmed by Figure 3 which shows that there are very high resonant peaks in the vicinity of the 5th and 7th harmonic. The magnitudes for the 5th and 7th harmonic are 0.0344074 per unit and 0.0127801 per unit respectively.

In order to minimize the voltage distortion that is produced by the converter, four additional capacitors of 0.5 per unit each are at first randomly placed at the network buses. The A matrix and the poles and zeros for the output response at bus 18 are calculated. The optimization algorithm as described in section 2.3, is applied, resulting in a neighborhood search over the configuration space.

Figure 4 shows the value of the objective function for each iteration. It can be seen that J increases with each iteration. The optimal capacitor assignment is obtained after five iterations. The maximum value of J is 0.96337 per unit. For this example the optimal response at bus 18 is obtained when additional capacitors are connected to the following buses: 2, 12, 16 and 17.

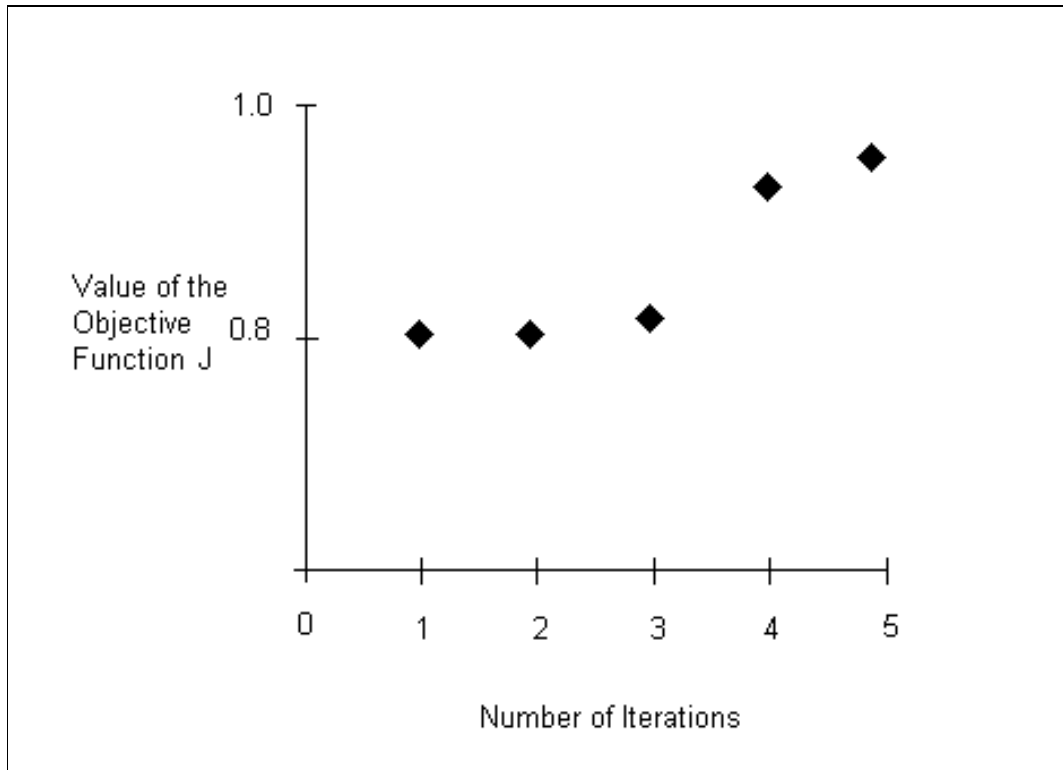


Figure 4: Value of the Objective Function for Each Iteration

The poles and zeros for the optimal configuration are shown in Table 3. The output response is shown in Figure 5.

Table 3: Lower system poles and zeros in per unit with the optimal capacitor assignment.

Poles	Lines
$\pm j16.6779$	$\pm j16.8447$
$\pm j11.2373$	$\pm j16.4566$
$\pm j7.98704$	$\pm j7.99356$
$\pm j5.96337$	$\pm j4.59542$
$\pm j3.96613$	0

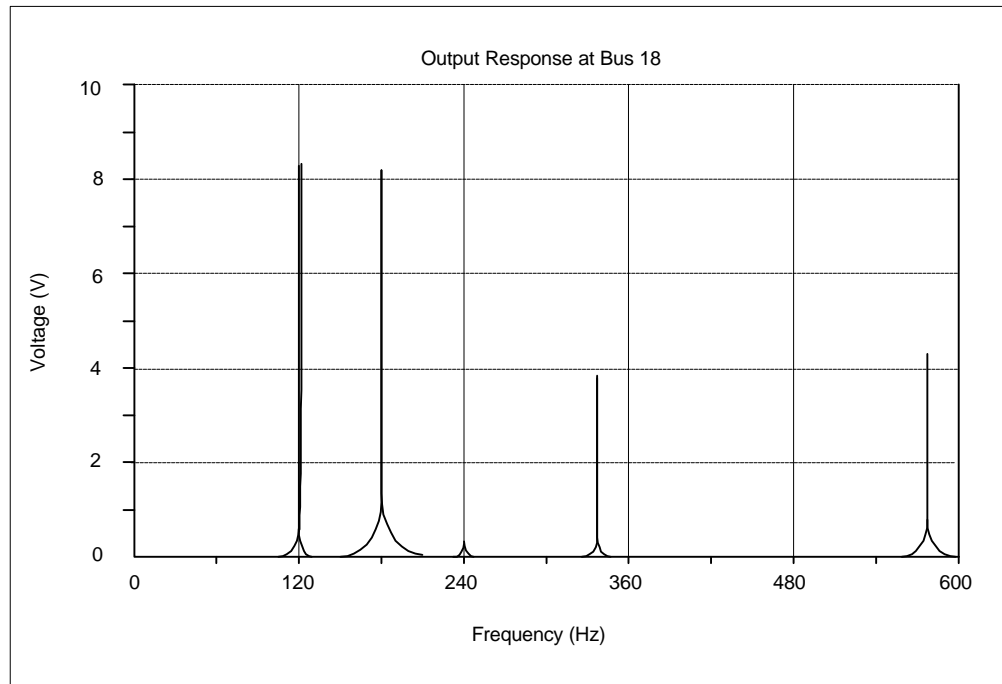


Figure 5: V-Harm® Output Response with the Optimal Capacitor Assignment

From Table 3 it can be seen that the nearest poles to the 5th and 7th harmonic are at 5.96337 and 7.98704 respectively. The frequency response of the simulation performed in V-Harm® also confirms the significant improvement over the original system. The magnitudes of the 5th and 7th harmonic are 0.00222821 per unit and 0.00708988 per unit respectively. This is an improvement by a factor of about 15 and 2 respectively.

The new network configuration is therefore better than the original distribution system in terms of harmonic distortion.

Conclusion

It has been shown in this paper, that the HDP can be formulated in terms of an optimization problem. The objective function and its constraint can be expressed in terms of differences between poles, zeros and harmonic current injections. The optimization algorithm was successfully applied to an 18 bus example network and the validity of the method was confirmed by V-Harm® simulations.

References

- [1] Arrillaga, J.; Bradley, D. and Bodger, D.: Power System Harmonics, John Wiley & Sons, New York 1985.
- [2] IEEE Tutorial Course: "Power System Harmonics" Course Text, 84 EHO221-2-PWR, 1984.
- [3] Ortmeyer, T.H. and Zehar, K.: "Distribution System Harmonic Design" IEEE Transactions on Power Delivery, Vol. 6, No. 1, pp. 289-294, January 1991.
- [4] Wickramasekara, M.G. and Lubekeman, D.: "Application of Sensitivity Factors for the Harmonic Analysis of Distribution System Reconfiguration and Capacitor Problems" Proceedings of the Third International Conference on Harmonics in Power Systems", pp 141-148, Purdue, September 1988.
- [5] Grady, W.M., Samotyj, M.J. and Joyola, A.H.: "The Application of Network Objective Functions for Actively Minimizing the Impact of Voltage Harmonics in Power Systems" IEEE Transactions on Power Delivery, Vol. 7, No. 3, pp. 1379-1386, July 1992.
- [6] Friedland, B.: Control System Design, McGraw-Hill, New York, 1987.
- [7] Fletcher, R.: Practical Methods of Optimization, John Wiley & Sons, Chichester, 1987.
- [8] V-Harm Users Manual: Power System Harmonics Simulation and Analysis Program, McGraw-Edison, Cooper Industries, May 1988.

Acknowledgments

We would like to thank Mr. S.S. Ahmed for his constructive contributions to this project.

H.V. Hitzeroth
A. Petroianu
University of Cape Town

Modeling Relay Operational Characteristics Using Electromagnetic Transients Program

Techniques Using EMTP to Model Dynamic Operations Characteristics of Distance Relays

Abstract

This paper highlights some techniques employed to model dynamic operational characteristics of distance relays using EMTP. Simulation results of a self- and a cross-polarized Mho relay are presented.

Keywords: EMTP Simulation, Power System Protection, Relay Modeling

Introduction

There are many commercially available software packages nowadays for power system analysis. These range from load flow, stability, contingency and reliability analysis. The Electro-Magnetic Transients Program is a widely used program for simulation and analysis of power system transients. The Transient Analysis Control Systems, the so-called (TACS) of the EMTP functions like an analogue computer. This allows signals to be passed between TACS and the electric network facilities simulated by EMTP. In fact, with TACS facilities it is possible to simulate control circuitry associated with rotating machinery, HVDC converters and static var controllers [1]. It is also possible to extend the application of EMTP to relay testing [2]. In such applications, simulated transients data can be created in ASCII format by EMTP and converted to analogue signals to be amplified for testing of relays. This approach is, however, an 'open-loop' type of simulation as the operation of relay can not alter the primary system configuration of system running arrangement. On the other hand, if relay models are simulated within the EMTP environment, then it becomes a 'close-loop' simulation as the operation of a particular relay, and thus the associated circuit breaker, would change the system conditions. Subsequent relay operations can then be further investigated. In this manner, dynamic operation of relays can be studied solely on a personal computer with no external hardware arrangement necessary. This paper describes the basic techniques used for simulation of distance relays, such as a self and cross-polarized distance relays commonly used for the protection of transmission circuits.

An Output Latching Relay

An instantaneous overcurrent relay is used to illustrate the basic techniques employed in the modeling of a latching relay which is used for the tripping of a circuit breaker. Instantaneous relays are simple relays which measure fault current flowing on the primary circuit and initiate tripping when the measured quantity exceeds some predetermined value. To model its operation, an ideal source in series with a lumped line impedance is set up as the primary system. A short circuit fault is applied to the system by employing a switch which connects the phase voltage direct to ground (or between phases, depending on the type of fault to be simulated) at the end of the line. To simulate the on/off operation of a circuit breaker, an arrangement using two SCR devices connected back to back is implemented. The on/off control of the circuit breaker is performed by a firing signal generated by the relay. Under normal conditions when the breaker is supposed to be 'close', a continuous positive firing pulse is presented to the SCRs. When the relay trips on overcurrent condition, a negative firing pulse is sent to the SCRs. To model the latching function of the relay output, two invertors and a summer are used. When the relay picks up on overcurrent condition, a signal "RELAY" with +1V is sent to the summer. This would cause "INV_2" to be at -1V and the "INV_1" to be at +1V. As the limiting value at "INV_2" is set between -2V and 0V, the latch finally settles at an output of -2V. This output signal then goes through another summer feed with a fixed constant input of +1.5V. It can be seen that when the relay picks up, a negative "CB" signal from the second summer (being $-2V + 1.5V = -0.5V$) is sent to the SCRs to open the breaker.

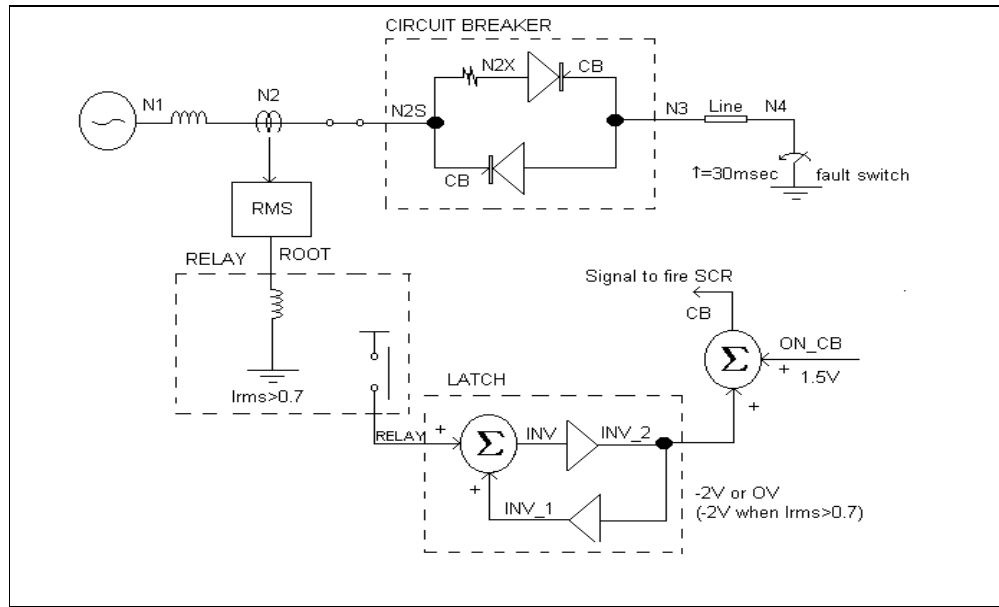


Figure 1: Modeling a Latching Relay

If the relay does not pick up, the latch output will stay at 0V while the “CB” signal will stay at +1.5V. This positive signal ensures the SCRs are continuously fired to maintain the breaker at the ‘close’ position. As for the relay’s operation, the sole criterion is that the current measured by the RMS detector being greater than a predetermined value. However, for the distance relay models described in the following section, the trip signal is injected directly at point ‘RELAY’ to control the circuit breaker.

Distance Relay Models

Self-Polarized Mho Relay

A self-polarized Mho characteristic based on phase-measuring technique as illustrated in Figure 2 is constructed. The two input signals to the relay are $V\angle -90^\circ$ and $V - IZ$, where $V\angle -90^\circ$ is the polarizing voltage (VP) taken from the relaying point, I is the current derived from the secondary of the line current transformer, and Z is the replica impedance of the relay. The operating criteria of the modeled relay being that $V\angle -90^\circ$ and $V - IZ$ are in phase for faults on the circumference of the Mho circle having IZ as its diameter. For in-zone faults, $V\angle -90^\circ$ leads $V - IZ$ as shown.

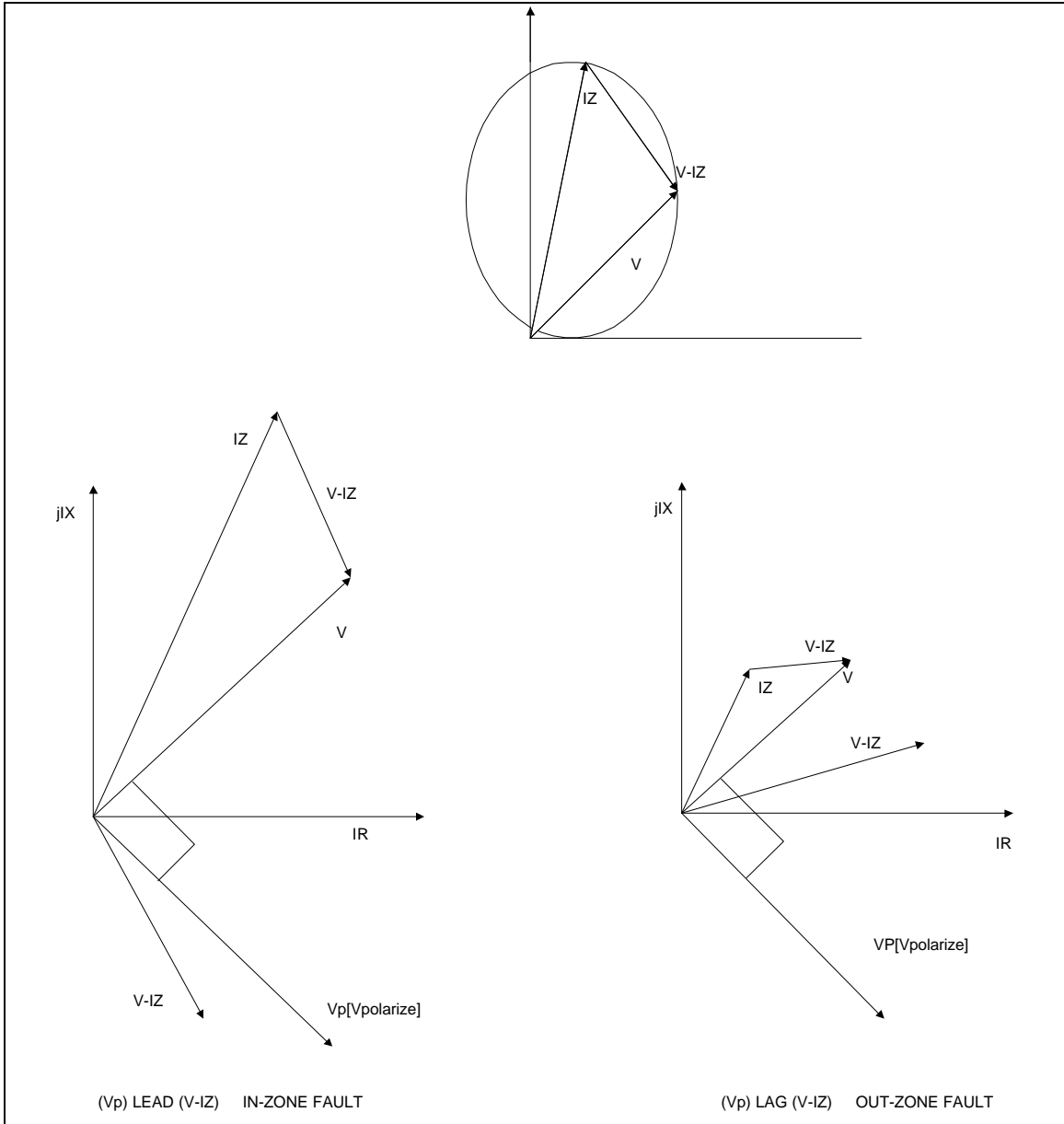


Figure 2: Vector Diagram of a Mho Relay

The simulation, including the primary system, is shown in Figure 3. The source of the electrical network is treated as an ideal source and Device 14 of the EMTP is conveniently used for this case. The phase-comparator is modeled using standard TACS devices available within the EMTP. The functioning of this comparator is discussed in section III.2. Referring to Figure 3, the device Z_{set} , connected across the secondary of the C.T., is the setting impedance of the relay being fixed at $0.144 \angle 79.88^\circ$ in the proposed simulation to match 100% of the line impedance. While the current signal is derived from N2sec and multiplied with Z_{set} to provide the signal IZ , the voltage signal is taken direct from the electric network at node N3. The 90 degree phase shift applied to the voltage is achieved by delaying the signal by 5 ms. The phase relationship of the two input signals VA and V3 is then

compared, and a trip signal 'TR' is given if signal VA lags V3 over a range from 0° to 180° . This criterion is checked by using some logical statements [3] provided by EMTP.

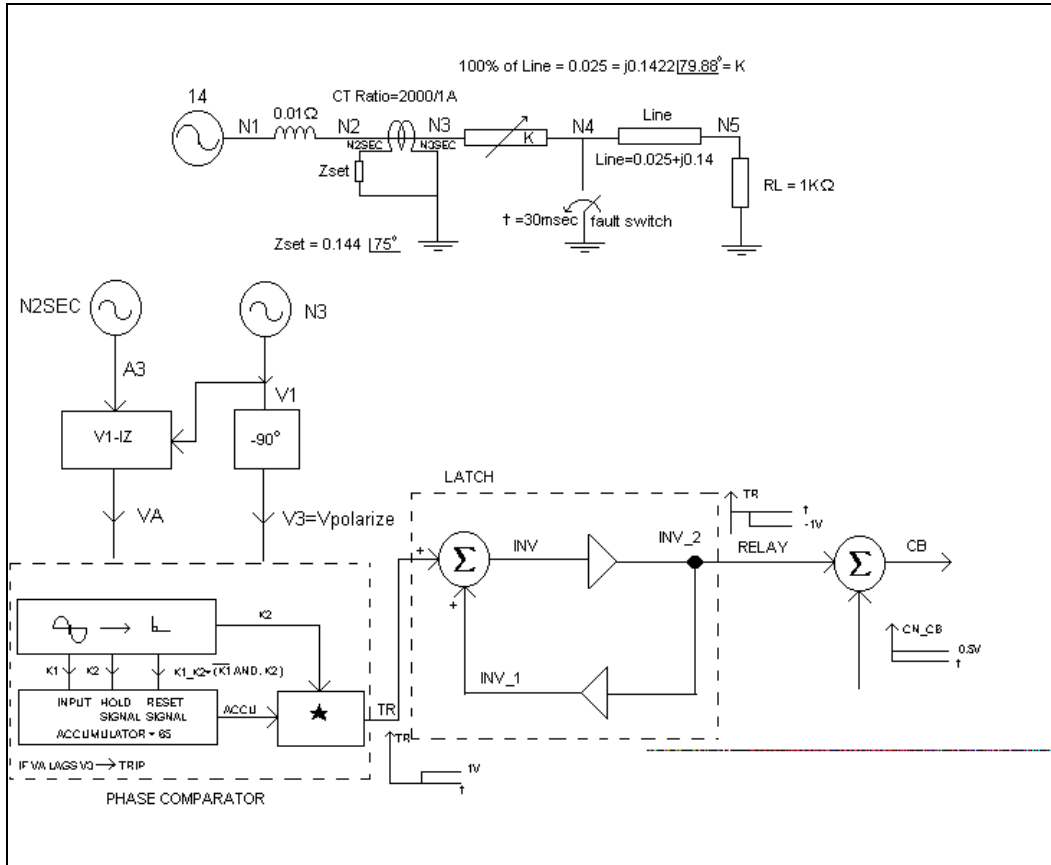


Figure 3: Simulation of a Mho Relay

The Phase Comparator

There is an accumulator device coded number '65' in the EMTP. This can be used to form the basic component of the phase comparator. In our application, the status of the accumulator is determined through the relationship of the input signals K1 and K2 representing VA and V3 respectively. As shown in Table 1, when both K1 and K2 are zero the output of the accumulator is zero, when K1 is zero and K2 is a logical '1', the output of the accumulator will be reset to zero. When K1 is 1 and K2 is zero, the output of the accumulator ramps up. The output will not change if both K1 and K2 are logical '1'. The final output of the phase comparator is determined by multiplying the output of the accumulator with the signal K2.

Table 1: Signals to the accumulator

K1	K2	O/P
0	0	0
0	1	Reset to 0
1	0	Ramps up
1	1	No change

Figure 4 shows the waveforms of the phase comparator. A trip 'TR' is generated when the signal K1 leads K2, as shown in the left hand part of the diagram. By adopting this arrangement, the operation of a phase comparator which measures the two input signals and provides a Mho relay characteristic is successfully modeled.

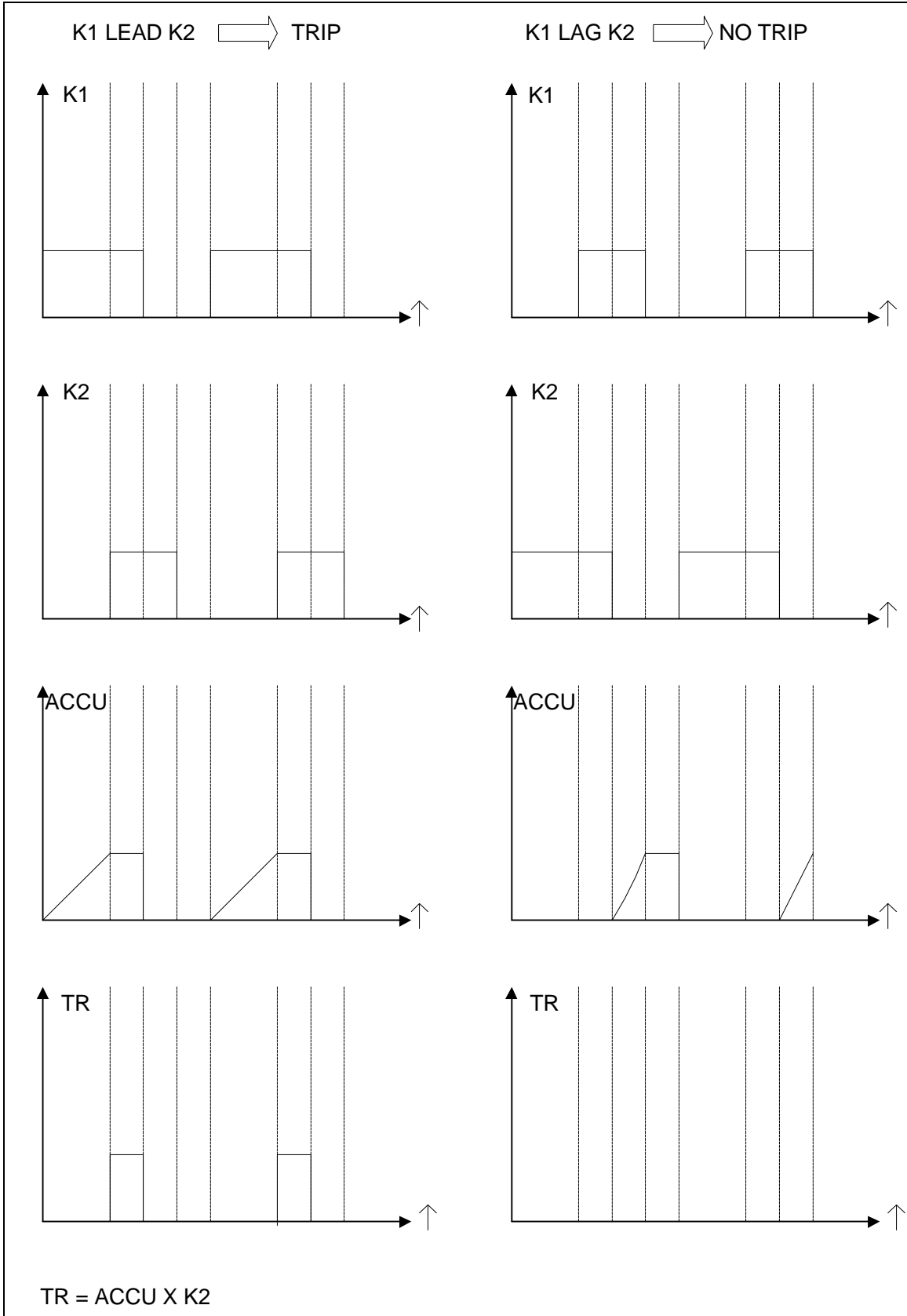


Figure 4: Internal Waveforms of Comparator

Tripping tests were simulated within the EMTP environment, where a fault of 95% and 105% respectively of the line length was applied to the network. Figure 5 shows the tripping output of the modeled relay for a fault at 0.95 p.u. along the protected line, while Figure 6 shows no tripping of the relay for a fault just outside the protected zone.

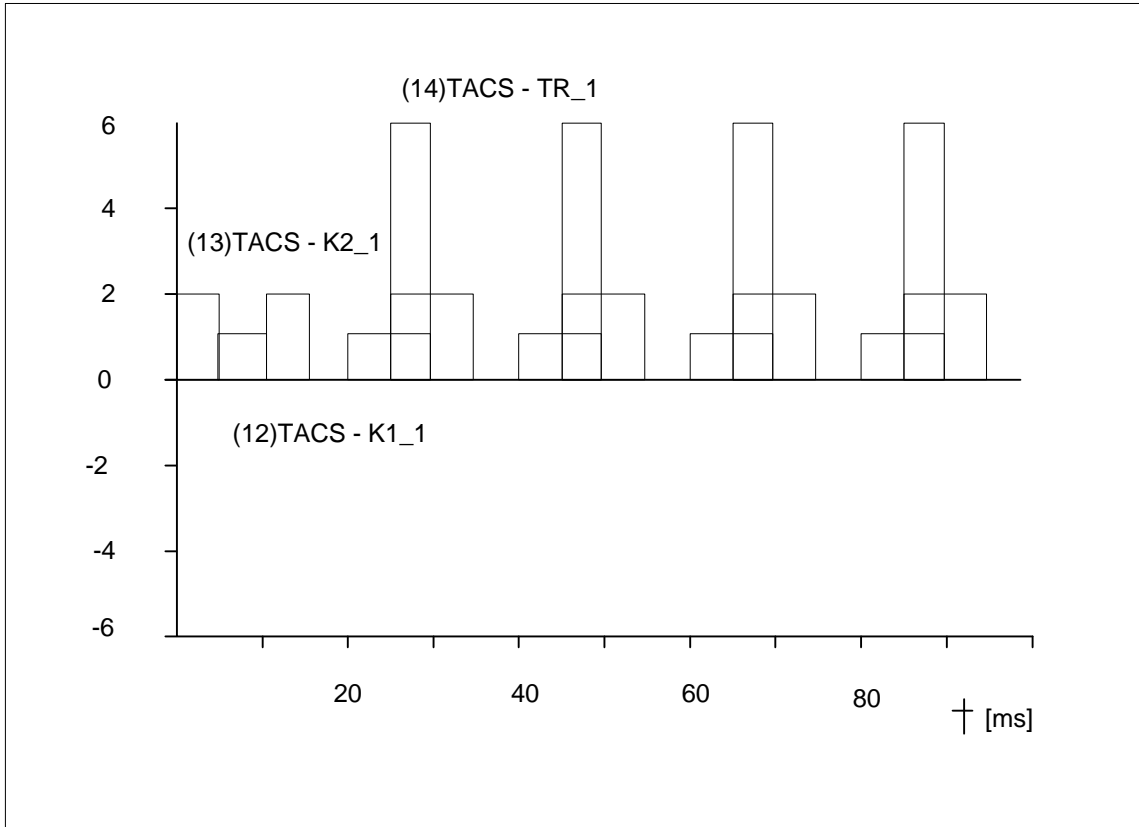


Figure 5: Comparator Output for an Internal Fault

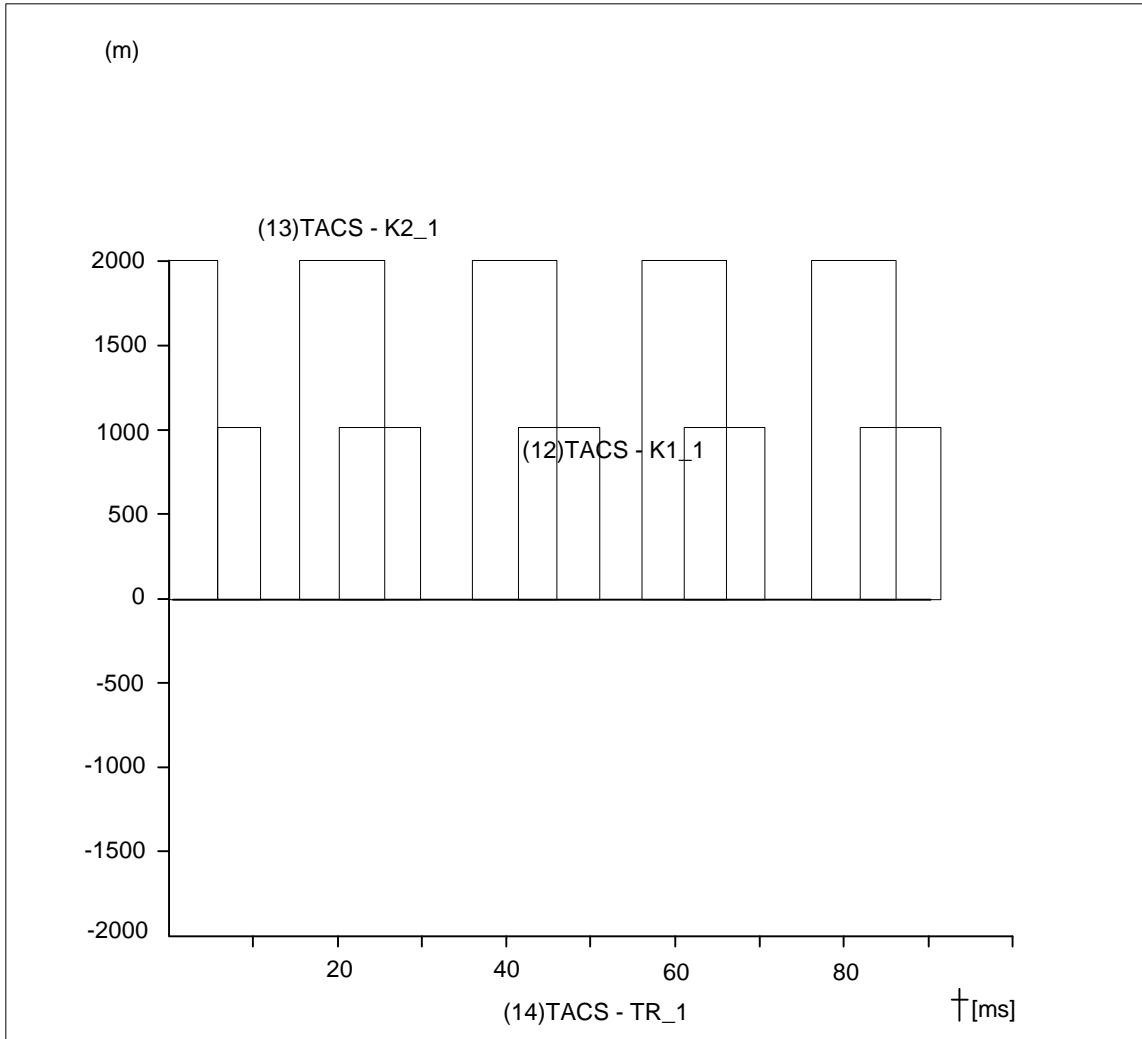


Figure 6: Comparator Output for an External Fault

Cross-Polarized Mho Relay

For cross-polarized relays, some partial health-phase components are used to maintain a correct polarizing signal for the relay under close-up faults. One approach [4] to derive the polarizing signal for 'A' -phase-to-ground fault is shown in Figure 7 where the cross-polarized signal is taken from the healthy phase 'BC'. In this arrangement, only 16% was required according to the design. For 'B'-phase-to-ground fault, the cross-polarizing signal would come from phase 'AC' and likewise for the others.

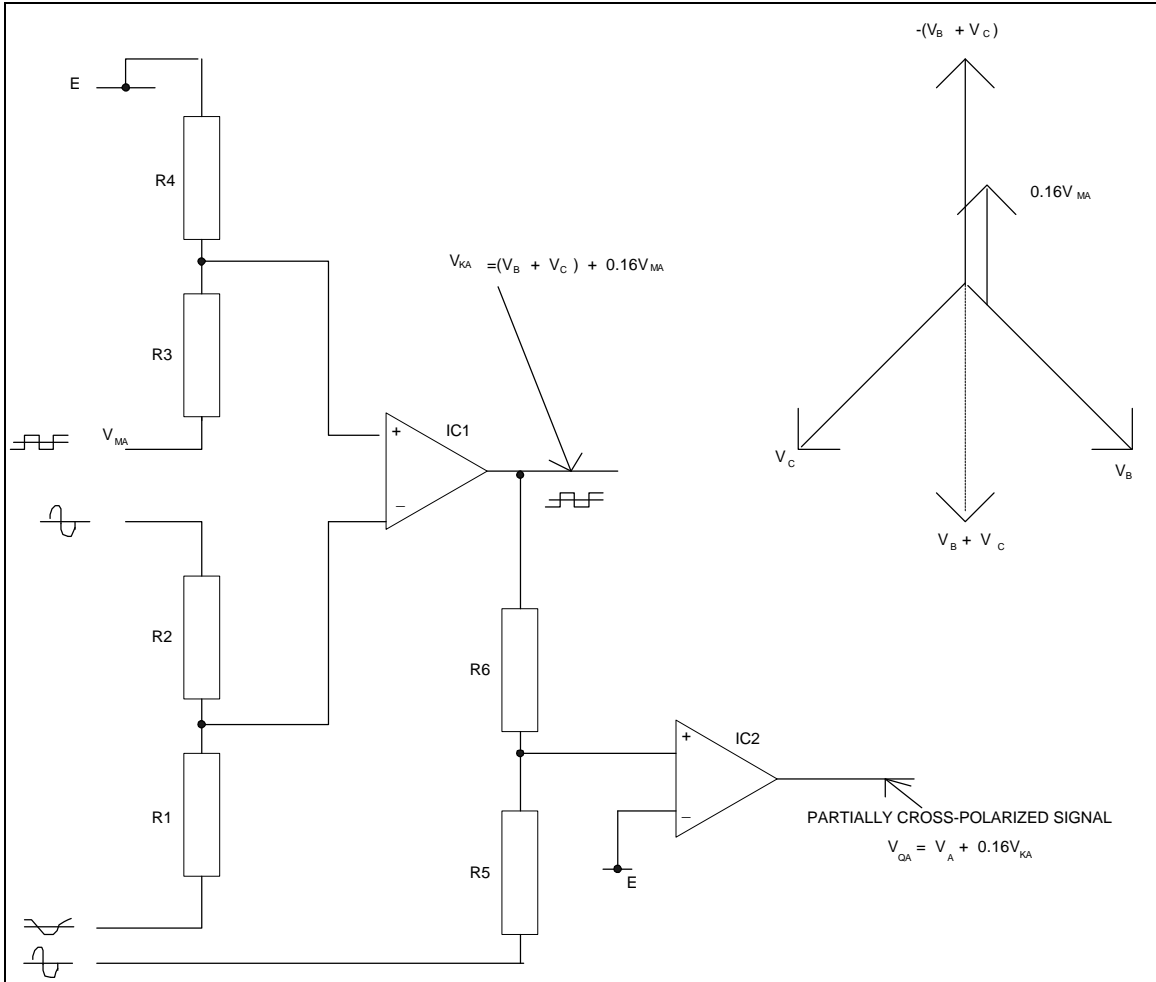


Figure 7: Cross-Polarizing Signal

The corresponding EMTP simulation with *p* - cable model is illustrated in Fig. 8. A phase-to-phase fault is applied to the network at an instant when $t=10\text{ms}$. In the relay model, the first 90° delay shifts the cross-polarizing signal to be in phase with the signal taken from the phases involving the fault, it is then added on to the overall polarizing signal before feeding to the phase comparator circuit.

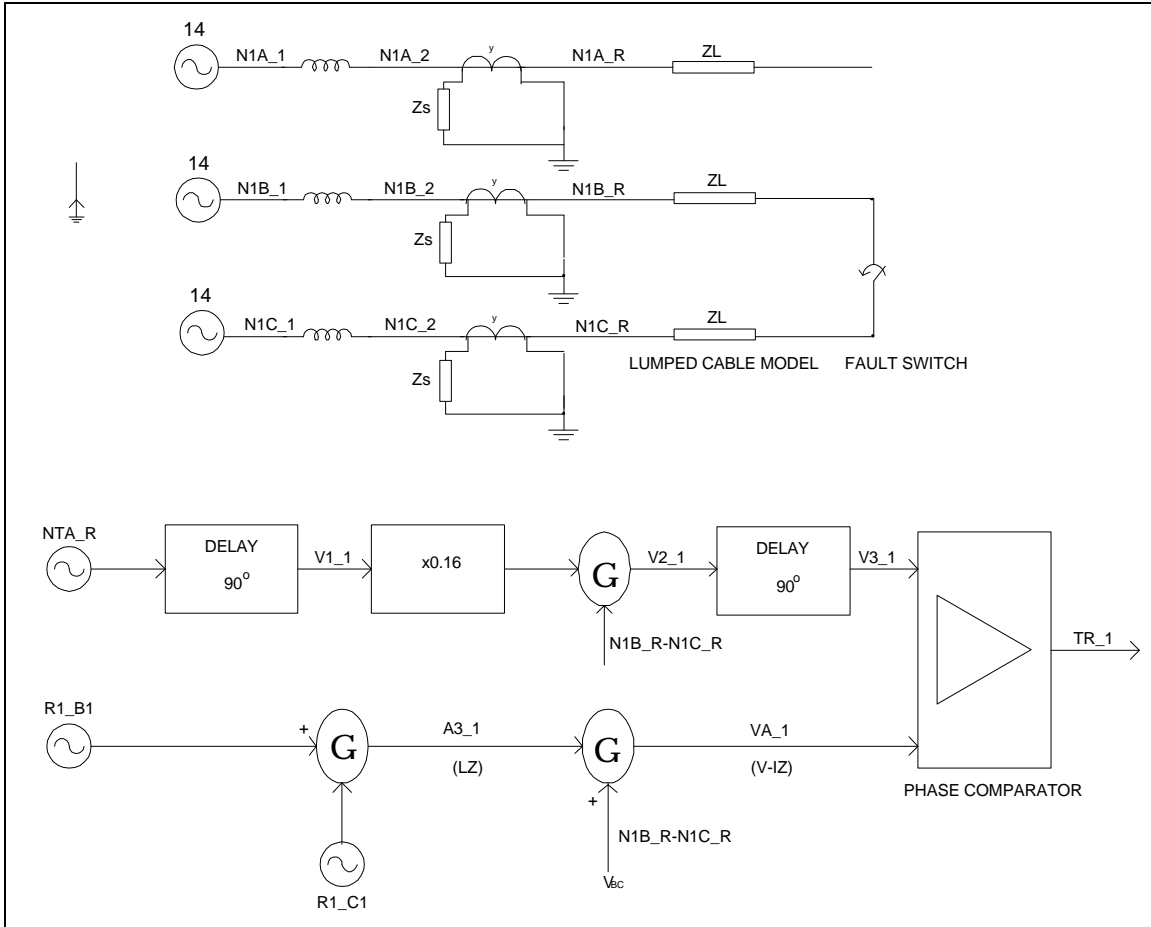


Figure 8: Modeling of a Cross-Polarized Mho Relay

An internal and external fault respectively was simulated on the network and the response of the relay model was observed to be correct as with the case of the self-polarized mode. This model was further tested on a three-source network to verify its directional characteristics under reverse fault condition. The primary system used for the investigation is as shown in Figure 9. In this simulation, there are a total of 6 relays as marked R1 to R6 on the network. The input signals required by relay R1 are derived from locations N1A_R, N1B_R, N1C_R, R1_B1 and R1_C1. While the corresponding signals for relay R2 would be N2A-R, N2B-R, N2C_R, R2_B1 and R2_C1.

A fault was applied to the network between node 1 and node 2 at a location 90% from node 1. The zone -1 reach of relay R1 is set to cover only 80% of the line length. Figure 10 shows the output of the comparator of each relay on the network. It can be seen that, for the fault as mentioned, only relay R2 provides a tripping signal since its input signal K1 leads K2. This confirms the directional feature relays R3 and R5 which should 'see' the fault being in the reversed direction.

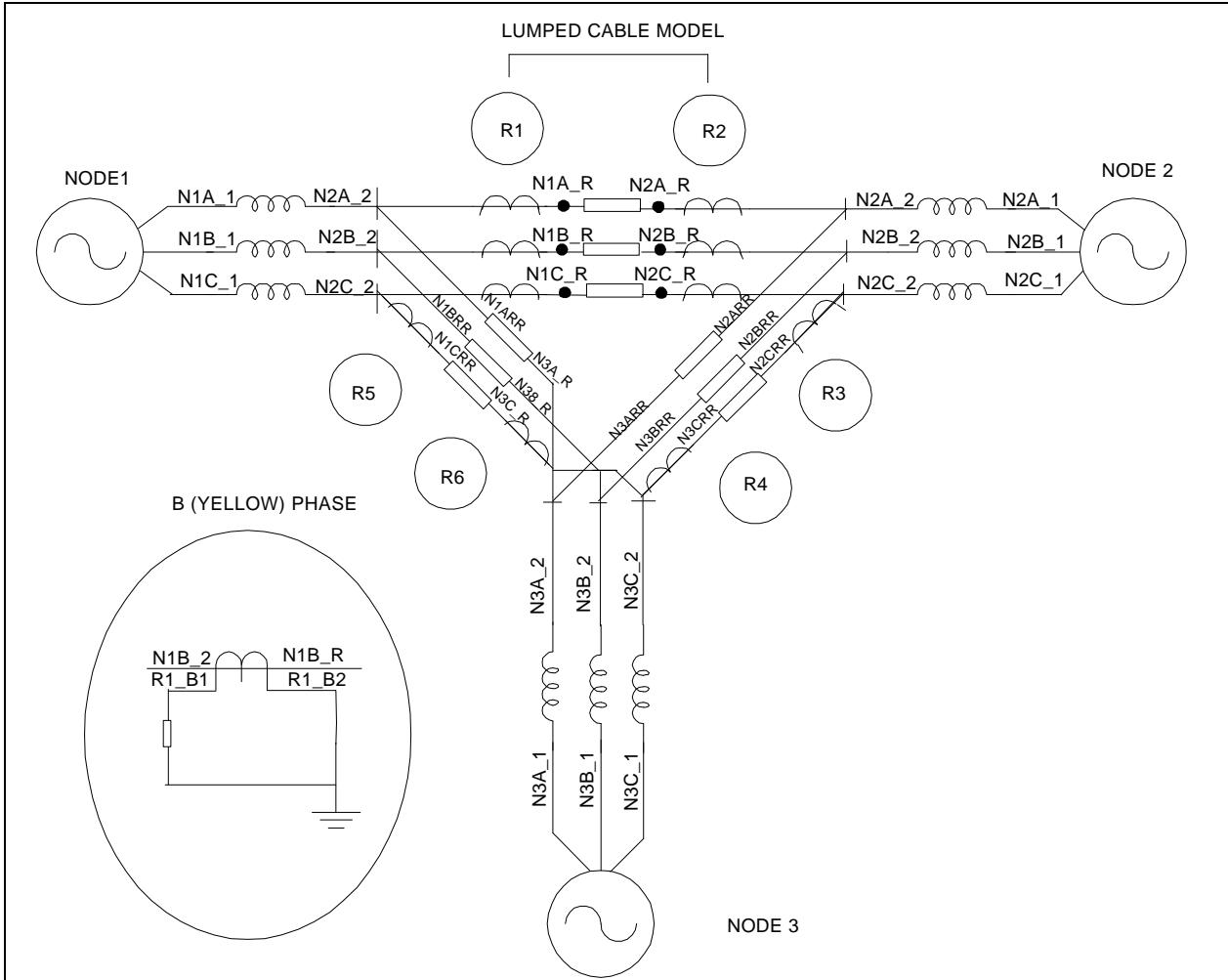


Figure 9: A Three-Source System for Testing Directional Characteristics

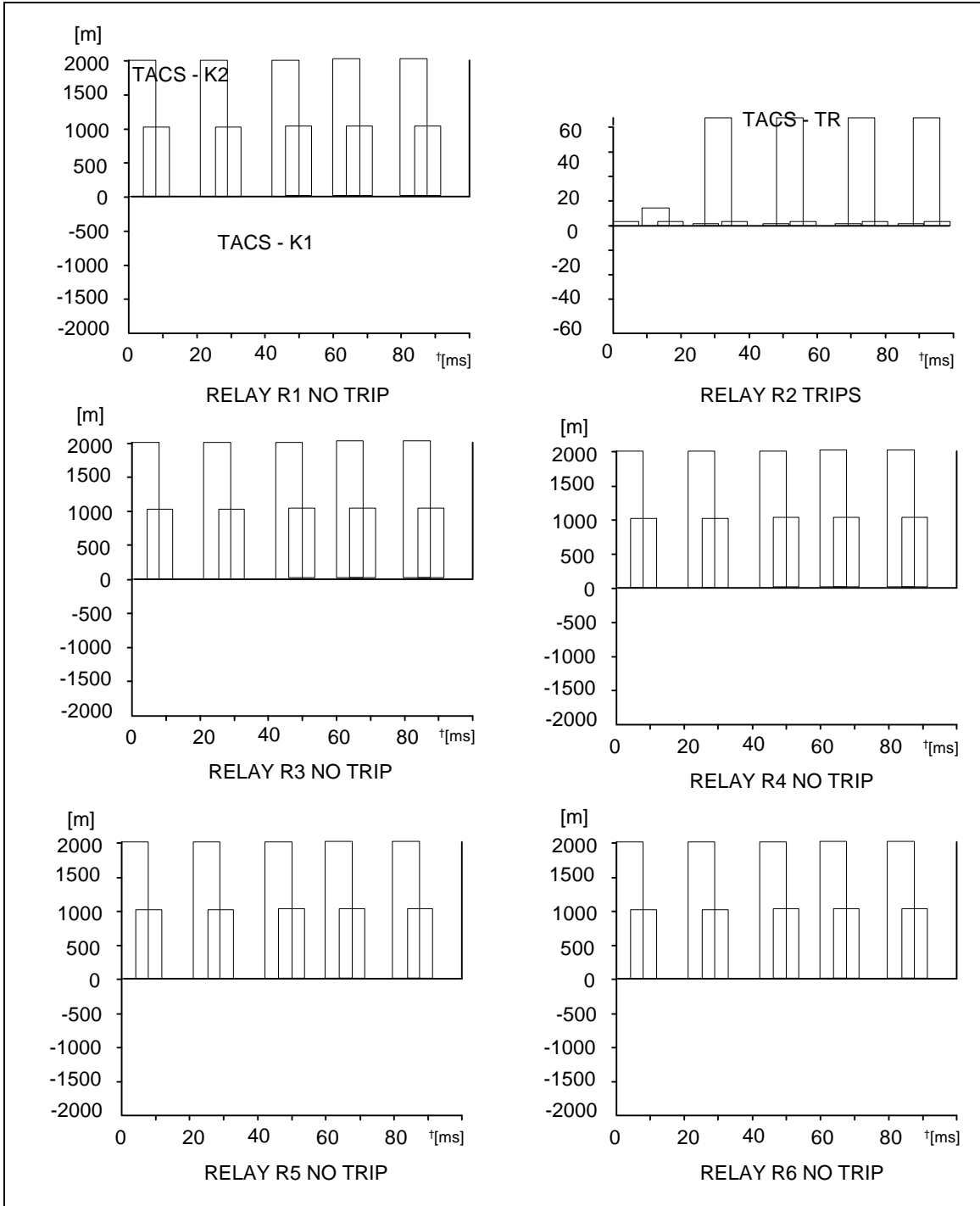


Figure 10: Simulated Output of Cross-Polarized Relay Model

Conclusions

Distance relays have been modeled using the EMTP program. The models are simple to implement using the TACS of the EMTP, and they are able to illustrate the operational characteristics of the modeled relay under different system conditions. All simulations are performed within the EMTP environment in a 'close-loop' fashion. The transients aspects of the CT and VT have not been dealt with in this paper, and they ought to be investigated. Since no source-code programming is required for the modeling, this approach should be of great help to those protection engineers who are not experienced programmers.

References

- [1] ElectroMagnetic Transients Program (EMTP) Revised Rule Book v.2. The EMTP DCG. 1989.
- [2] Wilson R.E., Nordstrom, "EMTP Transient Modeling of a Distance Relay and a Comparison with EMTP Laboratory Testing." IEEE Transactionns Power Delivery, Vol. 8, No. 3, July 1993.
- [3] Chan, T.W. et al, "Relay Models for ElectroMagnetic Transients Program," pp 534-539, Proceedings Stockholm Powertech, 18-22, June 1995.
- [4] GEC Measurements "Protective Relays Application Guide," Third Edition, 1987.

T.W. Chan
K.M. Chua
K.T. Lim
Nanyang Technological University
Republic of Singapore

Twelve-Pulse Cancellation and DC Motor Drives

Study Using SuperHarm® to Model Facility Power System to Determine Resonance Effects

Recently, I performed a study at an industrial plant that had an extensive number of dc motor drives. These drives are typically used on processes where speed control is very important. As a part of the overall study, SuperHarm was used to model the facility power system to determine the resonance effects of power factor correction capacitors installed on the site.

The user of SuperHarm must determine: how much of a system to model, how to model loads, and whether to build a single-phase equivalent or a complete three-phase representation. Correctly answering these questions involves experience and a physical understanding of the phenomena being studied. Seminars, first-hand experience, and learning from others through our Harmflo Users Group are ways to insure that these considerations are handled appropriately, with a minimum of effort. Problems where the analyst has the least experience require the most effort, because less simplification can be justified for the analysis.

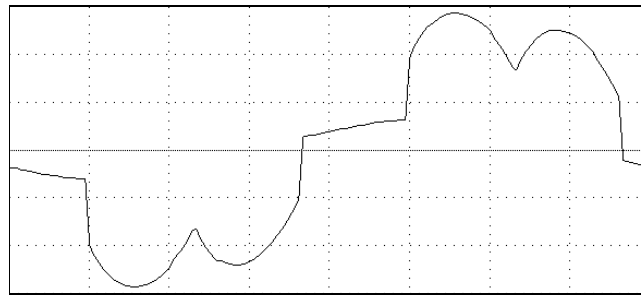
Many times a single-phase equivalent model is sufficient to study the harmonics resonance concerns of power factor correction capacitors. This simplification can reduce the effort needed for a study. However, this industrial plant had a variety of different transformer connections; some transformers used delta-wye windings, while other transformers used delta-delta windings. This mix of connections was installed to insure some cancellation of six-pulse harmonic currents. So a three-phase model was used in this study because the 12-pulse cancellation of the transformer connections was considered to be important in the analysis.

An important aspect to any computer simulation technique is the validation of the model. This validation will always involve measurements, either at the site being studied, or if it is a new installation, at a previous location studied that had similar characteristics. Measurement results were available for this particular site. One group of measurement results gave the total harmonic voltage distortion (THD_v) for the entire site with most of the load in operation. Another set of results showed that the (THD_v) declined as one large production line was idled. While it may seem an expected result that the THD_v would decline when the load was reduced, the initial results from SuperHarm model predicted that the THD_v should increase when this particular production line was idle. Why?

Further examination of the model showed that it expected that the operation of the large production line should produce harmonics currents that would cancel other six-pulse harmonic currents being generated at the facility. This

cancellation would be due to the combination of the various transformer winding arrangements. However, the analysis was refined when further measurements revealed that the large production line produced currents at a low displacement power factor. Unlike most AC variable frequency drives, DC motor drives operate at a variety of displacement power factors depending on operating conditions. This variation often allowed the 5th and 7th harmonics from the production line to combine, and not cancel as expected by the model.

Figure 1 below gives a current waveform and harmonic spectrum from the equipment (at a different site) with a large amount of dc drive load.



Event Number 70		Channel C		Setup 1		10/05/93		11:17:21.87	
Fnd:	183.61A	273 deg	18th:	0.1%	13 deg	35th:	1.9%	32 deg	
2nd:	0.9%	283 deg	19th:	2.1%	357 deg	36th:	0.0%	43 deg	
3rd:	0.3%	182 deg	20th:	0.1%	347 deg	37th:	1.2%	61 deg	
4th:	0.3%	170 deg	21st:	0.1%	116 deg	38th:	0.0%	162 deg	
5th:	24.8%	155 deg	22nd:	0.0%	181 deg	39th:	0.1%	125 deg	
6th:	0.3%	123 deg	23rd:	3.0%	229 deg	40th:	0.0%	172 deg	
7th:	2.4%	198 deg	24th:	0.1%	233 deg	41st:	1.7%	295 deg	
8th:	0.1%	303 deg	25th:	1.8%	252 deg	42nd:	0.1%	336 deg	
9th:	0.3%	275 deg	26th:	0.1%	265 deg	43rd:	1.2%	323 deg	
10th:	0.1%	284 deg	27th:	0.2%	27 deg	44th:	0.1%	321 deg	
11th:	7.8%	59 deg	28th:	0.1%	118 deg	45th:	0.0%	71 deg	
12th:	0.1%	64 deg	29th:	2.3%	132 deg	46th:	0.0%	153 deg	
13th:	2.4%	100 deg	30th:	0.1%	97 deg	47th:	1.5%	199 deg	
14th:	0.0%	175 deg	31st:	1.5%	155 deg	48th:	0.0%	203 deg	
15th:	0.1%	146 deg	32nd:	0.0%	265 deg	49th:	1.2%	222 deg	
16th:	0.1%	158 deg	33rd:	0.1%	272 deg	50th:	0.0%	257 deg	
17th:	4.4%	323 deg	34th:	0.0%	280 deg				
T.H.D.:		27.3%	ODD CONTRIB.:		27.3%	EVEN CONTRIB.:		1.1%	
Frequency: 50.0 Hz									

Figure 1: Waveform and Harmonic Spectrum Drawn by Equipment with a DCMotor Drive

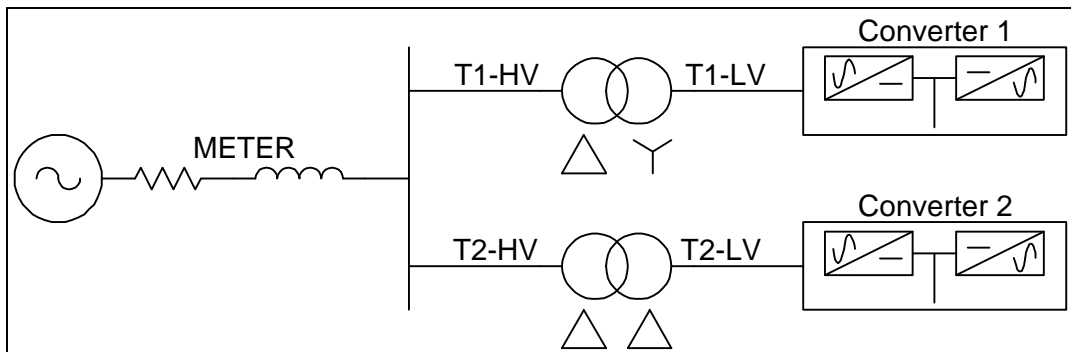
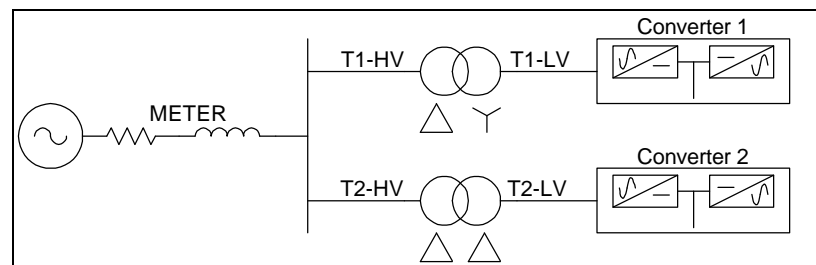


Figure 2: One-Line Diagram of a Twelve-Pulse System Model

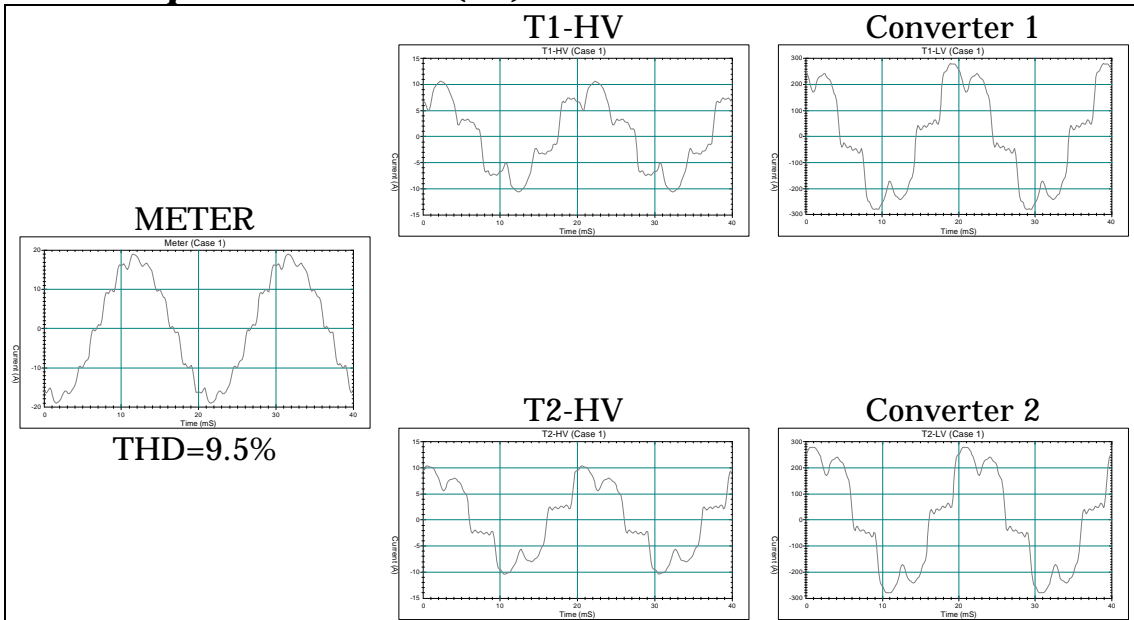
For a simple illustration of this effect a simple twelve-pulse cancellation model can be used as shown in Figure 2. A three-phase model is constructed, with one transformer having a delta-delta winding, and the other transformer was modeled delta-wye. The drive harmonic current was modeled as a nonlinear load. Note: When using Dranetz 658 spectrum data, the phase angles must be entered in as negative values, and the results must be viewed as a cosine series in TOP.

Two cases can demonstrate the phenomena. The first case was modeled with both drives at an identical operating point. The second case considered the effect of varying the displacement power factor angle of the second converter.

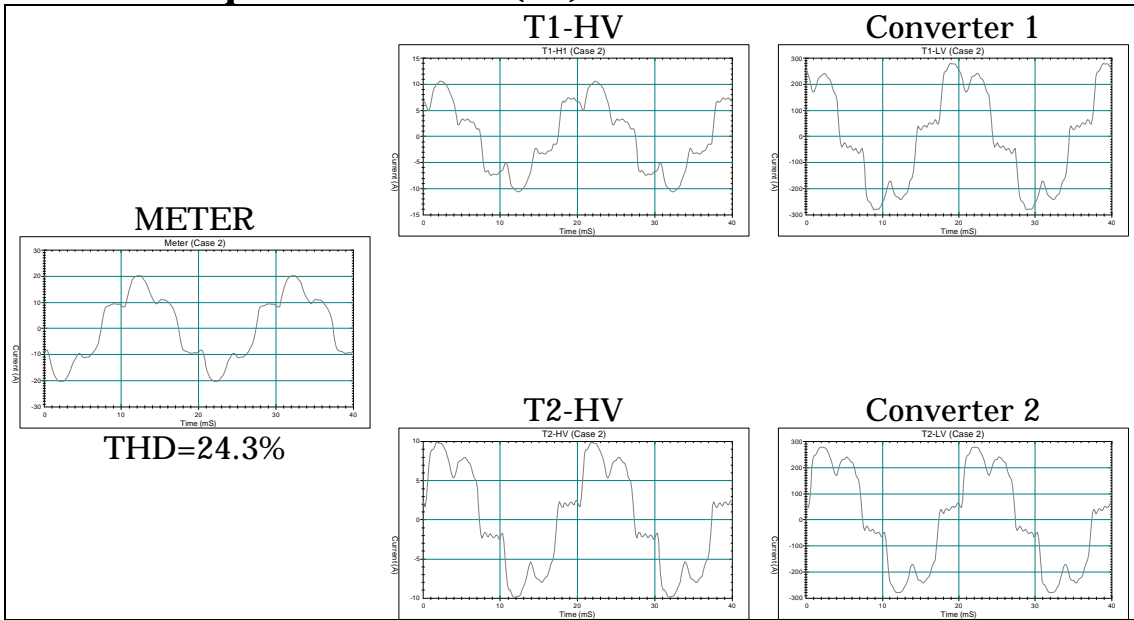
These results should convince the reader of the importance of varying displacement factor with d.c. motor drives. Failing to consider this effect could lead to overly optimistic (or pessimistic) results. An advantage of the SuperHarm program is the ease with which the user can modify the displacement factor in the nonlinear load model, when the program will automatically adjust the phase angles of all the harmonics.



**Simulation Case 1:
Same displacement factor (0.8) on both converters**



**Simulation Case 2:
Different displacement factor (0.5) on converter 2**



David R. Mueller
Senior Consultant
Electrotek Concepts, Inc.